Management and Production Engineering Review
Volume 17 • Number 1 • March 2026 • pp. 1–11
DOI: 10.24425/mper.2026.158638

Optimization of Printing Parameters for Direct and Indirect Extrusion on Hydrogel 3D Printers

Thanh Tan NGUYEN[1], Ngoc Hieu PHAM[1], Hoai Nam NGUYEN[1], Quoc Bao PHAN[2], Van Tron TRAN[1]

[1] *Ho Chi Minh City University of Technology and Engineering, Faculty of Mechanical Engineering, Vietnam*
[2] *Binh Duong University, Advanced Manufacturing Lab, Artificial Intelligence and Digital Transformation Institute, Vietnam*

Received: 28 February 2025
Accepted: 28 November 2025

Abstract
Three-dimensional (3D) printing is an attractive method for creating gel geometries for specific applications. In this research, the 3D printing parameters for direct and indirect extrusion of alginate-based hydrogels are optimized using the Taguchi and Analysis of Variance methods for output responses, including printed shape retention and the height of the 3-printed layers. The results show that for an indirect extrusion, the optimal values of extrusion speed, printing speed, and nozzle distance for the shape retention ability are 13 steps/mm, 50 mm/s, and 0.5 mm, respectively, while those values for the printed height are 13 steps/mm, 60 mm/s, and 0.5 mm, respectively. For direct extrusion, the optimal parameter set for former response is 35 steps/mm, 60 mm/s, and 0.6 mm, respectively, while the set for the latter is 35 steps/mm, 40 mm/s, and 0.6 mm, respectively. The findings in this report can be used as data for related research.

Keywords
Hydrogel, 3D printing, direct extrusion, indirect extrusion, optimization

Introduction

Hydrogels are three-dimensional and crosslinked networks of hydrophilic polymers that can absorb and retain large quantities of water or biological fluid, yet not dissolve. This special characteristic makes them similar to living tissues. Therefore, hydrogels have enormous potential for applications in the medical field, such as the replacement of load-bearing organs, cell and tissue engineering, wound-care products, and drug delivery systems (Lee & Mooney, 2001; Yang et al., 2012; Jeon et al., 2016; Hsieh et al., 2017). Moreover, recently developed hydrogels exhibit other prominent properties, including excellent mechanical performances, high electrical and thermal conductivity, and rapid self-recovery. Thus, they can also be applied in the engineering fields (Sun et al., 2012; Malischewski et al., 2016; Ji et al., 2022). Hydrogels can be divided according to many factors, such as origin, polymer composition, molecular network structure, activation ability, electrical conductivity of the network, physical aspect, and chain configuration (Fig. 1) (Tran et al., 2020a; Tran et al., 2020b; Tran, 2024).

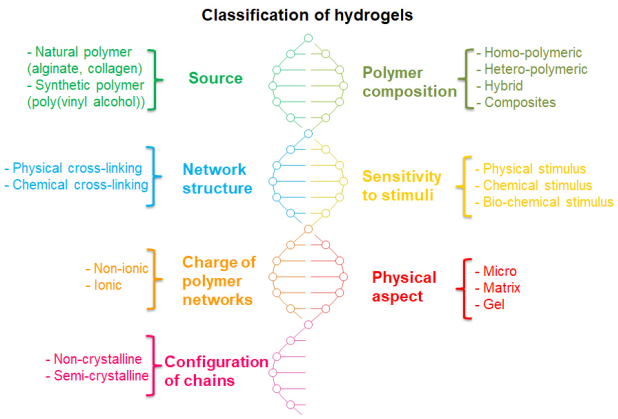

Fig. 1. Classification of hydrogels.

Recent reports have demonstrated that there have been several methods for shaping hydrogels, such as casting, three-dimensional (3D) printing, and welding

***Corresponding author**: Van Tron Tran – Ho Chi Minh City University of Technology and Engineering, Faculty of Mechanical Engineering, Vietnam, Postal Address:Ho Chi Minh City University of Technology and Engineering, Faculty of Mechanical Engineering, Ho Chi Minh City, 70000, Vietnam, phone: (+84) 914146826, e-mail: trontv@hcmute.edu.vn*

(Tran et al., 2018; Mredha et al., 2018; Liu et al., 2023; Caprioli et al., 2021; Dhand et al., 2025; Tran et al., 2024b; Tran, 2025a; Le & Tran, 2025). In the casting method (Tran et al., 2018; Tran et al., 2020b), a mold with a cavity in the shape of the designed part is first created. Afterward, a gel precursor solution is filled into the cavity and then solidifies into a gel. Finally, the mold is opened, and the gel part in the desired shape is obtained. For 3D printing (Caprioli et al., 2021), generally, the geometry is first designed using computer-aided design (CAD) software. Subsequently, the design is sequentially exported into stereolithography (STL) and G-code format files. The code file is then transferred to a 3D printer, which contains a gel precursor solution serving as a printing ink. Thereafter, the ink is printed layer by layer following the file. The printed solution is finally gelated to achieve the intended gel geometry. For the welding technique, the crosslinks of ionically physical hydrogels are first degraded in a specific monovalent salt solution, leading to the free state of the backbone polymers (Tran et al., 2024b; Tran, 2025a). Then the gels are allowed to absorb welding additive polymer chains. Finally, the hydrogels are re-crosslinked to obtain the desired welding structures. Among these methods, 3D printing is known as a novel method for rapidly shaping various materials in 3D structures with extraordinary production efficiency (Goyanes et al., 2019; Jiang et al., 2019a; Van Damme et al., 2020; Singamneni et al., 2021, Jain et al., 2021; Kaliampakou et al., 2023; Le & Tran, 2025; Tran, 2025a). Thus, it has been applied in many industries. Recently, many attempts have been made to apply this additive manufacturing method for gel materials (Jiang et al., 2019a; Van Damme et al., 2020; Jain et al., 2021; Kaliampakou et al., 2023).

Alginate-based hydrogels, fabricated using alginate – a biopolymer extracted from brown seaweeds – have been regarded as outstanding materials for numerous applications in both biomedical and engineering fields since they exhibit advantageous properties such as eco-friendliness, biocompatibility, biodegradability, and ease of fabrication (Tran et al., 2023). Recently, various studies focusing on manufacturing structures of the hydrogels via the printing technique have been introduced (Xiong et al., 2023; Khan et al., 2024; Tran, 2025b). For example, Österberg and co-workers successfully applied the 3D printing technique to fabricate 3D scaffolds using spherical colloidal lignin particles and cellulose nanofibril-alginate hydrogel. The research investigated the printed possibility of various gel compositions by varying the ratio of colloidal lignin particles and cellulose nanofibril (Zhang et al, 2020). In other research, Cao and co-workers studied the potential of using alginate-chitosan polyion complex hydrogels to produce complicated shapes of scaffolds for tissue engineering (Khan et al., 2024). The study also evaluated the shape fidelity of the printed structures by changing the content of chitosan (Khan et al., 2024). Furthermore, Doyle and co-workers demonstrated the optimum composition of alginate and gelatin in the alginate-gelatin hydrogels for 3D bioprinting. As reported, the blend of 7% alginate and 8% gelatin was proposed as the optimum (Xiong et al., 2023).

The Taguchi method employs orthogonal tables for experimentation and yields reliable data. The Taguchi model is effective when the number of components ranges from 3 to 50. The Taguchi technique is mostly utilized during the parametric design phase, focusing on the analysis and evaluation of the influence of factors on output parameters, while simultaneously identifying the ideal configuration of technological parameters. Experimental processes frequently exhibit complexity, with numerous input factors influencing the output variable either separately or collectively, and the output is represented in various amounts. One-input, one-output models are incapable of demonstrating the concurrent impact of factors on output, hence unilaterally portraying processes (Ghaderinejad et al., 2021).

Although numerous studies have explored the use of 3D printing techniques to create structures from alginate-based hydrogels, recognizing the effect of various printing parameters, such as printing speed, feed rate, and printing distance, on the quality of printed products (Tabriz et al., 2015; Zhang et al., 2020). However, there has been a notable lack of research on evaluating the influence of printing parameters, including extrusion speed, printing speed, and nozzle distance, on the shaping of the gels during printing. To address those technical gaps, this study aimed to determine printing parameters for various output factors, such as printed shape retention and product height, for both direct and indirect extrusions of our developed 3D printing machine. This study used an alginate solution made by dissolving 5 wt.% of Na-alginate in distilled water. Some statistical methods, such as Taguchi and Analysis of Variance (ANOVA), were employed for optimization.

Materials & Methods

- Material
  Sodium alginate (Na-alginate, viscosity 80–120 cP) was purchased from FUJIFILM Wako Pure Chemical Corporation, Japan. Calcium chloride ($CaCl_2$) was purchased from Samchun Pure Chemical Co., Ltd., Republic of Korea. Activated

charcoal was purchased from Duchefa Biochemie, Netherlands. All chemicals were used as received without further purification. Distilled water was used to prepare the gel.

- Preparation of precursor alginate aqueous solution
  To prepare a 5 wt% Na-alginate precursor solution for printing, a mixture of distilled water and food coloring was first prepared in a 97:3 volume ratio. Subsequently, 5 g of Na-alginate was weighed into a glass jar, followed by the addition of 95 g of the aqueous mixture. The resulting solution was then stirred periodically, twice daily, for approximately three days until a homogeneous printing precursor was obtained.
- Machine
  The 3D printing machine for hydrogel material was developed by a previous research based on the recently reported working principle. The machine was built using commercial hardware and control software with the parameters shown in Fig. 2 (direct and indirect extrusion). The calculation, design, and manufacturing of the machine were detailed and reported in our late paper (Nguyen et al., 2024). The 3D printing process is shown in Fig. 3.

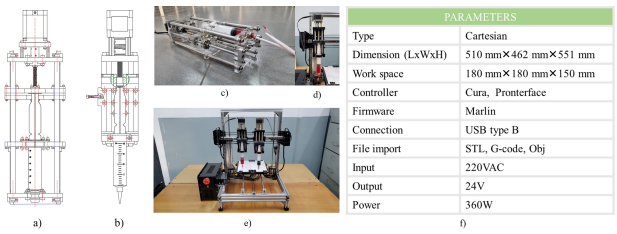

PARAMETERS	
Type	Cartesian
Dimension (LxWxH)	510 mm×462 mm×551 mm
Work space	180 mm×180 mm×150 mm
Controller	Cura, Pronterface
Firmware	Marlin
Connection	USB type B
File import	STL, G-code, Obj
Input	220VAC
Output	24V
Power	360W

Fig. 2. Indirect extrusion (a and c), direct extrusion (b and d), 3D printing machine (e), and parameter of a 3D printing machine (f) (Nguyen et al., 2024).

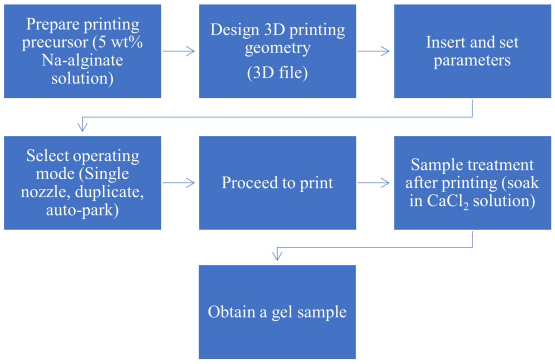

Fig. 3. Diagram of the 3D printing process of alginate-based hydrogel.

Taguchi and ANOVA Methods

The Taguchi method was applied to optimize the parameters of a 3D printer. An L9 experimental design was used to investigate the influence of three factors: Extrusion speed (steps/mm), Print speed (mm/s), and nozzle distance, with three levels for both indirect and direct extruders, with the following parameters, respectively: 9, 11, 13; 40, 50, 60; 0.5, 0.7, 0.9 and 30, 35, 40; 40, 50, 60; 0.5, 0.55, 0.6. The output results, Shape retention time (s), and printed height (mm) were collected using calipers and a stopwatch. The data were analyzed using Minitab 19 software (Minitab LLC, State College, United States). Analysis of variance (ANOVA) and the Signal-to-Noise (S/N) ratio were used to determine the influential factors and optimal levels

– Experiment process: The optimal experiments were carried out as follows.

Step 1: Identify input and response objects.

- Input objects: extrusion speed (steps/mm), printing speed (mm/s), and distance to nozzle (mm).
- Response objects: Shape retention time (s) and height for 3 =printed layer (mm).

Step 2: Determine the levels of the input factor. In this study, 3 levels of each input factor were selected based on the capacity of the fabricated printing machine (Tab. 1).

Table 1
Levels of direct and indirect extruders.

Parameter	Indirect extruder			Direct extruder		
	Level 1	*Level 2*	*Level 3*	*Level 1*	*Level 2*	*Level 3*
Extrusion speed (steps/mm)	9	11	13	30	35	40
Printing speed (mm/s)	40	50	60	40	50	60
Distance to nozzle (mm)	0.5	0.7	0.9	0.5	0.55	0.6

Step 3: Determine the appropriate orthogonal array for optimization.

To select the orthogonal array, the total degrees of freedom (DOF) were calculated. With 3 variables and 3 levels for each, the DOF was calculated as shown in Tab. 2. Since the DOF was 7, the L9 orthogonal array was chosen in this study.

Step 4: Assign values to the L9 orthogonal array (Tab. 2)

Table 2
Variables and degrees of freedom in the experiment.

Variable	Degrees of Freedom
Overall average	1
A, B, C	$3 \cdot (3-1) = 6$
Interaction between two variables	0
Total	$1+6+0=7$

Step 5: Conduct experiments and collect data

Step 6: Analyze experimental results and optimize

The larger the better where:

- y_u: the value of the u^{th} measurement
- n: number of experiments in the orthogonal array

Results and Discussion

In this study, the three input parameters, including extrusion speed, printing speed, and nozzle distance, were optimized for the output responses, such as shape retention and printed height, during the printing process of alginate solution using both indirect and direct extruders. These factors were selected since they are consistently identified in the literature as the most influential parameters governing material flow, layer adhesion, and dimensional accuracy in extrusion-based additive manufacturing (Tabriz et al., 2015; Liu et al., 2018; Zhang et al., 2020). The factor levels (Tab. 1) were determined based on (i) the recommended operating ranges of our developed printing system, (ii) preliminary experiments conducted to identify stable and feasible intervals, and (iii) ranges commonly used in previous related studies. These considerations ensure that the selected factors and levels adequately represent the practical and functional design optimization of the printing process. For the optimization process, Taguchi and ANOVA methods and Minitab software were employed. The alginate solution was printed layer by layer, consisting of three distinct layers. Shape retention refers to the duration during which the three printed layers maintained their form on the printing plane (XOY plane), while printed height, measured using a digital caliper, indicates the thickness of these three layers (Fig. 4).

Influence of technological parameters of the indirect extruder on shape retention ability and printed height.

The experimental results obtained for the indirect extruder are shown in Tab. 3.

Fig. 4. (a) Average height of 3 layers (b) Shape retention time.

Shape retention time

The S/N ratio results displayed in Tab. 3 were obtained using the Taguchi optimization method with Minitab software. The signal-to-noise table of product image retention time is shown in Tab. 4 as a ratio effect chart. The S/N ratio of the product image retention time is presented in Fig. 5.

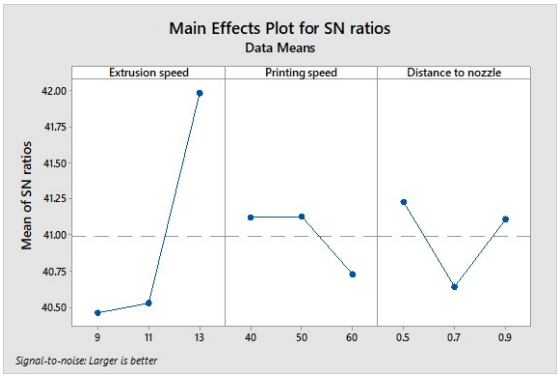

Fig. 5. S/N ratio of shape retention time.

The results indicated that the extrusion speed is the greatest influence on the technological parameter, with a Delta value of 1.53, followed by Distance to nozzle with a Delta value of 0.59, and the technology parameter has the least effect with a Delta value of 0.40.

To evaluate the influence of the technological parameters of the indirect extruder on product shape retention time, the ANOVA method is used. The results of running ANOVA on Minitab software are shown in Tab. 5.

The F-value is an important index in variance analysis and is used to evaluate the meaningful differences between technological parameters. Tab. 5 shows that extrusion speed is the most influential factor with a value of (6.09), followed by distance to the nozzle, and printing speed has values of 1.00), and (0.05), respectively.

P-value is an important index to evaluate the statistical significance of results. Tab. 5 shows that the value of extrusion speed is the smallest at 0.057, which means that this parameter has the most influence on the statistical results. Distance to the nozzle and printing speed have values of (0.363) and (0.834), respectively, which means that these two parameters do not significantly affect the optimization process.

Table 3
Experimental results with the indirect extruder and S/N ratio.

No.	Extrusion speed (Steps/mm)	Print speed (mm/s)	Nozzle distance (mm)	Shape retention time (s)			S/N	Printed height (mm)			S/N
				Experiment				*Experiment*			
				1	*2*	*3*		*1*	*2*	*3*	
1	9	40	0.5	109	115	101	40.658	1.4	1.2	1.4	2.428
2	9	50	0.7	108	102	103	40.360	1.2	1.3	1.2	1.803
3	9	60	0.9	102	107	104	40.363	1.2	1.1	1.2	1.316
4	11	40	0.7	107	102	104	40.363	1.4	1.4	1.5	3.113
5	11	50	0.9	108	108	106	40.6137	1.3	1.4	1.3	2.483
6	11	60	0.5	106	108	108	40.613	1.8	1.8	1.9	5.256
7	13	40	0.9	129	133	131	42.343	1.4	1.5	1.4	3.113
8	13	50	0.5	136	117	149	42.411	2	2.1	2.1	6.298
9	13	60	0.7	112	113	120	41.201	1.9	1.8	1.8	5.256

Table 4
Signal-to-noise ratio of product image retention time.

Level	Extrusion speed (steps/mm)	Printing speed (mm/s)	Distance to nozzle (mm)
1	40.46	41.12	41.23
2	40.53	41.13	40.64
3	41.99	40.73	41.11
Delta	1.53	0.40	0.59
Rank	1	3	2

Table 5
ANOVA analysis of variance on product image retention time.

Source	DF	Adjss	AdjMS	F-value	P-value	Contribution (%)
Extrusion speed	1	36.2702	36.2702	6.09	0.057	50.15
Printing speed	1	0.2893	0.2893	0.05	0.834	0.40
Distance to nozzle	1	5.9738	5.9738	1.00	0.363	8.26
Error	5	29.7840	5.9568			41.19
Total	8	72.3173				100.00

Optimize product retention time

Based on the percentage contribution of each factor to the variation of the data, it is found that extrusion speed contributes 50.15% to the variation, while the distance from the print head to the table (Distance to the nozzle) and printing speed (Printing speed) contribute 8.26% and 0.4%, respectively.

In addition, to find the relationship between factors affecting product image retention time, through ANOVA analysis of variance, a linear regression function was found:

Regression

$$T = 96.93 + 1.229\ \text{Extrusion speed} - 0.0220\ \text{Printing speed} - 4.99\ \text{Distance to nozzle} \quad (1)$$

Based on the linear regression equation, it is found that the extrusion speed is proportional to the product image retention time, while the distance from the print head to the table (distance to the nozzle) and printing speed are inversely proportional to shape retention time.

Through the above-analyzed data and observing Fig. 5, the optimal set of technological parameters of product image retention time can be drawn. The above optimal result also coincides with the set of parameters with sample 8 in Tab. 3 (extrusion speed: 13, printing speed: 50, nozzle distance: 0.5).

For the printed height of 3 layers

The S/N ratio results of the printed height shown in Tab. 6 were achieved via Taguchi analysis with Minitab software. The results are presented in Fig. 6.

Table 6
3-layer height signal-to-noise ratio of the product.

Level	Extrusion speed (steps/mm)	Printing speed (mm/s)	Distance to nozzle (mm)
1	1.85	2.885	4.661
2	3.618	3.528	3.391
3	4.889	3.943	2.304
Delta	3.040	1.058	2.357
Rank	1	3	2

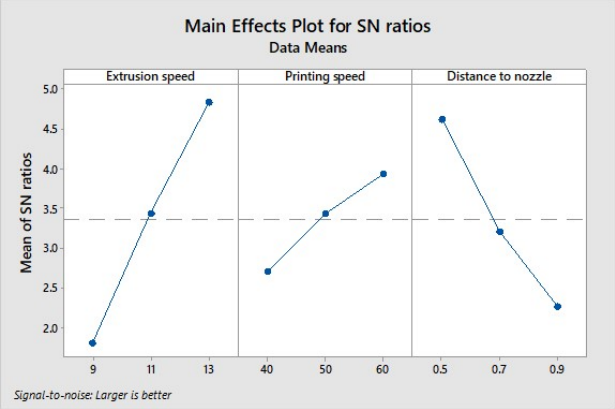

Fig. 6. Height of 3 layers.

The signal-to-noise ratio of the technological parameters of the extruder indirectly affects the 3-layer height of the product. Extrusion speed is the most influential factor, with a Delta value of 3.040, followed by the distance from the print head to the table (Distance to the nozzle) with a Delta value of 2.357, and the technology parameter that least affects the 3-layer height of the product is printing speed, with a Delta value of 1.058.

To evaluate the influence of technological parameters of the extruder on the 3-layer height of the product, the ANOVA method is used. The results of running ANOVA on Minitab software are shown in Tab. 7.

The F-value is an important index in variance analysis and is used to evaluate the meaningful differences between technological parameters. From Tab. 7, it can be seen that extrusion speed is the most influential factor with a value of 181.89, followed by the distance to the nozzle and printing speed, with values of 120.08 and 28.50, respectively.

Table 7
ANOVA analysis of variance for the 3-layer height of the product.

Source	DF	Adjss	AdjMS	F-value	P-value	Contribution (%)
Extrusion speed	1	0.42667	0.426667	181.89	0.000	54.22
Printing speed	1	0.06685	0.0066852	28.50	0.003	8.50
Distance to nozzle	1	0.28167	0.281667	120.08	0.000	35.79
Error	5	0.01173	0.002346			1.49
Total	8	0.78691				100.00

P-value is an important index to evaluate the statistical significance of results. Tab. 7 shows that the value of extrusion speed and Distance to the nozzle is the smallest at 0.000, which means that this parameter has the most effect on the statistical results. Printing speed has a value of 0.003, which means that this parameter does not affect the process of optimizing the 3-layer height of the product.

Based on the percentage contribution of each factor to the variation of the data, it is found that Extrusion speed contributes 54.22% to the variation, while the distance to the nozzle and printing speed contribute 35.79% and 8.50%, respectively.

In addition, to find the relationship between factors affecting the 3-layer height of the product, through ANOVA analysis of variance, a linear regression function was found:

Regression

$$\begin{aligned} H = {} & 0.282 + 0.13333 \text{ Extrusion speed} \\ & + 0.01056 \text{ Printing speed} \\ & - 1.0833 \text{ Distance to nozzle} \end{aligned} \tag{2}$$

Table 8
Set of 3-layer optimal technology parameters of the product.

Input		
Extrusion speed (steps/mm)	Printing speed (mm/s)	Distance to nozzle (mm)
13	60	0.5

Table 9
Experimental results of the direct extruder.

No.	Extrusion speed (Steps/mm)	Print speed (mm/s)	Nozzle distance (mm)	Shape retention time (s)			S/N	Printed height (mm)			S/N
				Experiment				*Experiment*			
				1	*2*	*3*		*1*	*2*	*3*	
1	30	40	0.5	105	102	104	40.310	1	1	1	0.000
2	30	50	0.55	110	112	113	40.956	0.95	0.95	0.95	–0.445
3	30	60	0.6	118	120	119	41.510	1.1	1.2	1.1	1.065
4	35	40	0.55	124	120	122	41.724	1	0.95	0.97	–0.240
5	35	50	0.6	124	130	127	42.071	1.2	1.2	1.2	1.583
6	35	60	0.5	123	125	130	42.000	0.95	1	1	–0.153
7	40	40	0.6	126	120	123	41.792	1.1	1.2	1.2	1.316
8	40	50	0.5	125	120	124	41.794	1	0.95	0.97	–0.240
9	40	60	0.55	120	126	125	41.839	0.95	1	1	–0.153

From the linear regression equation, it is found that the extrusion speed and printing speed are proportional to the 3-layer height of the product and the nozzle distance. Inversely proportional to the 3-layer height of the product.

Through the above analysis and observation of Fig. 6, the optimal set of technological parameters for the product's 3-layer height can be drawn (Tab. 8).

Influence of technological parameters of the direct extruder on shape retention ability and printed height.

Experimental results obtained for the direct extruder are shown in Tab. 9.

The S/N ratio results for the shape retention time when printing an alginate solution with the direct extruder are shown in Tab. 10. The results were achieved via Taguchi analysis using Minitab software. The results are presented in Fig. 7.

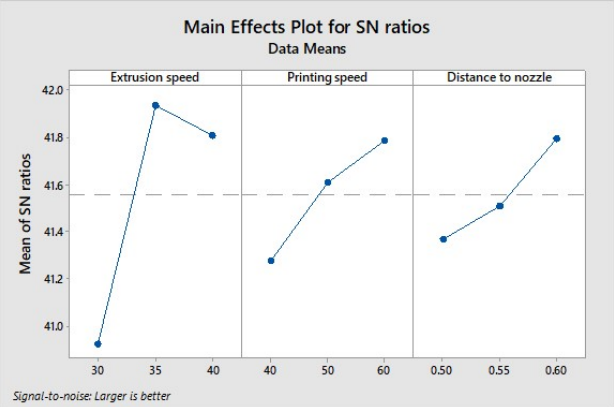

Fig. 7. S/N ratio of product image retention time.

Table 10
Signal-to-noise ratio of shape retention time.

Level	Extrusion speed (steps/mm)	Printing speed (mm/s)	Distance to nozzle (mm)
1	40.93	41.28	41.37
2	41.93	41.61	41.51
3	41.81	41.78	41.79
Delta	1.01	0.51	0.42
Rank	1	2	3

It is found that the extrusion speed is the most influential technological parameter on the output response, with a Delta value of 1.01, followed by Printing speed with a Delta value of 0.51. The technology parameter that has the least effect on product image retention time is the distance from the print head to the table (Distance to nozzle), with a Delta value of 0.42.

To evaluate the influence of technological parameters of the direct extruder on product shape retention time, the ANOVA method was used. The obtained results are shown in Tab. 11.

The F-value is an important index in variance analysis and is used to evaluate the meaningful differences between technological parameters. Tab. 11 shows that extrusion speed is the most influential factor with a Delta value of 7.52, followed by printing speed and distance from the print head to the table, which have the values of 2.41 and 1.41, respectively.

Table 11
ANOVA analysis of variance of product image holding time.

Source	DF	Adjss	AdjMS	F-value	P-value	Contribution (%)
Extrusion speed	1	208.07	208.07	7.52	0.041	45.47
Printing speed	1	66.67	66.67	2.41	0.181	14.57
Distance to nozzle	1	44.46	44.46	1.61	0.261	9.72
Error	5	138.35	27.67			30.24
Total	8	457.56				100.00

P-value is an important index to evaluate the statistical significance of results. Tab. 11 shows that the P-value of extrusion speed is the smallest at 0.041, suggesting that this parameter has the most effect on the shape retention of the printed gels. Printing speed and Distance to nozzle have values of 0.181 and 0.261, respectively, which means that these two parameters have less effect on the output factor.

Based on the percentage contribution of each factor to the variation of the data, it was found that Extrusion speed contributes 45.47% to the variation, while Printing speed and distance from the beginning, and distance to the nozzle, contribute 14.57% and 9.72%, respectively.

In addition, to find the relationship between factors affecting product image retention time, through ANOVA analysis of variance, a linear regression function was found:

Linear regression equation

$$T = 32.1 + 1.178 \text{ Extrusion speed} + 0.333 \text{ Printing speed} + 54.4 \text{ Distance to nozzle} \quad (3)$$

From the linear regression function, it is found that the technological parameters extrusion speed, printing speed, and distance from the print head to the Tab. 12 (Distance to nozzle) are proportional to the product holding time.

Through the above evidence and observing Fig. 7 S/N ratio, the optimal set of technological parameters for product image retention time can be drawn.

For the printed height of 3 layers

The S/N ratio results obtained using the Taguchi method with Minitab software are shown in Tab. 13.

Table 12
Optimal set of technological parameters for shape-holding time.

Input		
Extrusion speed (steps/mm)	Printing speed (mm/s)	Distance to nozzle (mm)
35	60	0.6

The 3-layer height S/N ratio of the product is presented in Fig. 8.

Table 13
Signal-to-noise ratio for the 3-layer height of the product.

Level	Extrusion speed (steps/mm)	Printing speed (mm/s)	Distance to nozzle (mm)
1	0.2066	0.3588	-0.1314
2	0.3965	0.2992	-0.2799
3	0.3075	0.2527	1.3220
Delta	0.1898	0.1060	1.6019
Rank	2	3	1

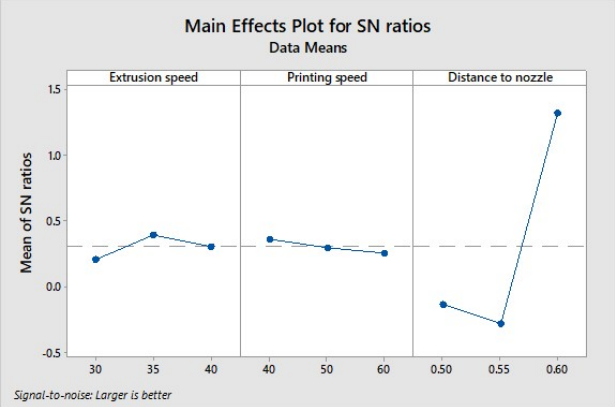

Fig. 8. S/N ratio of the product's 3-layer height.

The signal-to-noise ratio of the technological parameters of the extruder directly affects the 3-layer height of the product. Nozzle distance is the technological parameter that has the greatest influence, with a Delta value of 1.6019, followed by extrusion speed with a Delta value of 0.1898 and printing speed with a Delta value of 0.1060.

The ANOVA method was employed to evaluate the influence of the technological parameters of the direct extruder on the 3-layer height of the product, and the results achieved are shown in Tab. 14.

Table 14
ANOVA analysis of variance for the 3-layer height of the product.

Source	DF	Adjss	AdjMS	F-value	P-value	Contribution (%)
Extrusion speed	1	0.00267	0.000267	0.05	0.829	3.54
Printing speed	1	0.00267	0.000267	0.05	0.829	3.54
Distance to nozzle	1	0.049202	0.049202	9.6	0.027	65.28
Error	5	0.025630	0.005126			34.01
Total	8	0.075365				100.00

The F-value is an important index in variance analysis and is used to evaluate the meaningful differences between technological parameters. Tab. 14 shows that the Distance to the nozzle is the most influential factor with a value of 9.6, followed by extrusion speed and printing speed, respectively, with values of 0.05 and 0.05, respectively.

P-value is an important index to evaluate the statistical significance of results. From Tab. 14, it can be seen that the Distance to nozzle value is the smallest at 0.027, which means that this parameter has the most influence on the statistical results. Extrusion speed and Printing speed have values of 0.829 and 0.829, respectively, which means that these two parameters have less effect compared to the Distance to the nozzle.

Based on the percentage contribution of each factor to the variation of the data, it is found that the Distance to the nozzle contributes 65.28% to the variation, while the extrusion speed and printing speed contribute 3.54%.

In addition, to find the relationship between factors affecting the 3-layer height of the product, through ANOVA analysis of variance, a linear regression function was found:

Linear regression equation

$$\begin{aligned} H = {} & 0.031 + 0.00133 \text{ Extrusion speed} \\ & - 0.00067 \text{ Printing speed} \\ & + 1.811 \text{ Distance to nozzle} \end{aligned} \tag{4}$$

Based on the linear regression equation, it was found that the extrusion speed and the Distance to the nozzle are proportional to the 3-layer height of the product, and the printing speed is proportional to the product's 3-layer height.

Through the above evidence and observing Figure 8, the optimal set of technological parameters for the product's 3-layer height can be drawn.

Table 15
Set of technological parameters for optimal 3-layer height of the product.

Input		
Extrusion speed (steps/mm)	Printing speed (mm/s)	Distance to nozzle (mm)
35	40	0.6

The optimal input printing parameters for the direct extruder were used to create tensile test specimens in accordance with ASTM D638 standard type V (inset of Fig. 9a). The printed gels were subsequently crosslinked with 0.5 M Ca^2 for 1 day and then rinsed in water for an additional 1 day to obtain the required printed specimens. The specimens were subsequently evaluated with a commercial tensile tester (PT-1699vdo, PRO TEST, Taiwan) and a 50-kg load cell. The acquired tensile characteristics are presented in Figures 9a–c. The Young's modulus, tensile strength,

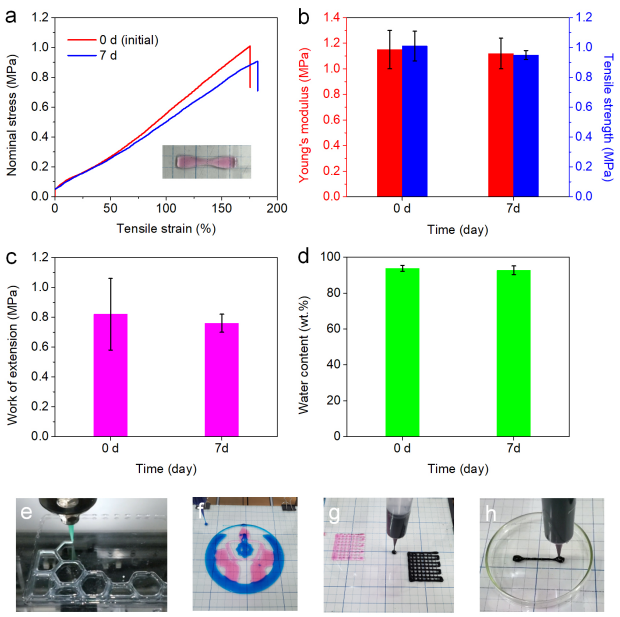

Fig. 9. (a) Representative tensile stress-strain curves of the printed hydrogels prepared using a 5 wt.% alginate precursor solution. The inset shows the printed tensile specimen. (b) Young's modulus and tensile strength, (c) work of extension, and (d) water content of the resulting hydrogels. Error bars in plots (b)–(d) indicate the mean absolute deviation ($n = 3$). (e–h) Various structures were printed using the optimal parameter sets of the indirect (e) and direct extruders (f–h).

and work of extension of the printed specimens were measured as 1.15 ± 0.15 MPa, 1.01 ± 0.1 MPa, and 0.82 ± 0.24 MJ·m^3 (Figures 9a–c), respectively, which are comparable to recently reported values (Tran, 2024; Mredha et al. 2018; Tran et al., 2024) Moreover, the tensile characteristics of the printed hydrogels were effectively preserved in water for 7 days (Figures 9a–c). Additionally, the parameter sets obtained for both extruders were effectively utilized to print diverse shapes (Figures 9e–h), particularly for the high-viscosity material composed of alginate and activated charcoal at concentrations of 5 wt.% and 2 wt.%, respectively.

Conclusions

In this study, the printability of the high-viscosity alginate-based solution was demonstrated, and the optimum printing parameters – extrusion speed, printing speed, and nozzle distance – for achieving the desired output responses of shape retention and printed height were determined while printing a 5 wt.% alginate solution using both the developed indirect and direct extruders. The results indicated that for the indirect extruder, the optimal input parameters for shape retention were 13 steps/mm, 50 mm/s, and 0.5 mm, while for printed height, the optimal values were 13 steps/mm, 60 mm/s, and 0.5 mm, respectively. For the direct extruder, the optimum parameter sets were 35 steps/mm, 60 mm/s, and 0.6 mm, and 35 steps/mm, 40 mm/s, and 0.6 mm for those output responses, respectively. However, the optimization process was carried out using a specific alginate precursor solution and our fabricated 3D printing system. It is necessary to determine optimal parameter sets for alginate-based precursor solutions with different viscosities, and the optimal parameter sets should be applied to other printing systems to further evaluate our results.

Acknowledgments

This work was supported by Ho Chi Minh City University of Technology and Engineering, Ho Chi Minh City, Vietnam.

References

Caprioli, M., Roppolo, I., Chiappone, A., Larush, L., Pirri, C.F., & Magdassi, S. (2021). 3D-printed self-healing hydrogels via Digital Light Processing. *Nature communications*, *12*(1), 2462. DOI: 10.1038/s41467-021-22802-z

Dhand, A.P., Davidson, M.D., & Burdick, J.A. (2025). Lithography-based 3D printing of hydrogels. *Nature Reviews Bioengineering*, *3*(2), 108–125. DOI: 10.1038/s44222-024-00251-9

Ghaderinejad, P., Najmoddin, N., Bagher, Z., Saeed, M., Karimi, S., Simorgh, S., & Pezeshki-Modaress, M. (2021). An injectable anisotropic alginate hydrogel containing oriented fibers for nerve tissue engineering. *Chemical Engineering Journal*, 420, 130465. DOI: 10.1016/j.cej.2021.130465.

Goyanes, A., Allahham, N., Trenfield, S.J., Stoyanov, E., Gaisford, S., & Basit, A.W. (2019). Direct powder extrusion 3D printing: Fabrication of drug products using a novel single-step process. *International journal of pharmaceutics*, 567, 118471. DOI: 10.1016/j.ijpharm.2019.118471

Hsieh, F.Y., Tao, L., Wei, Y., & Hsu, S.H. (2017). A novel biodegradable self-healing hydrogel to induce blood capillary formation. *Npg Asia Materials*, *9*(3), e363. DOI: 10.1038/am.2017.23

Jain, T., Tseng, Y.M., Tantisuwanno, C., Menefee, J., Shahrokhian, A., Isayeva, I., & Joy, A. (2021). Synthesis, rheology, and assessment of 3D printability of multifunctional polyesters for extrusion-based direct-write 3D printing. *ACS Applied Polymer Materials*, *3*(12), 6618–6631. DOI: 10.1021/acsapm.1c01275

Jeon, I., Cui, J., Illeperuma, W.R., Aizenberg, J., & Vlassak, J.J. (2016). Extremely stretchable and fast self-healing hydrogels. *Advanced Materials*, *28*(23), 4678–4683. DOI: 10.1002/adma.201600480

Ji, D., Park, J.M., Oh, M.S., Nguyen, T.L., Shin, H., Kim, J.S., Kim, D., Park, H.S. & Kim, J. (2022). Superstrong, superstiff, and conductive alginate hydrogels. *Nature Communications*, *13*(1), 3019. DOI: 10.1038/s41467-022-30691-z

Jiang, Z., Erol, O., Chatterjee, D., Xu, W., Hibino, N., Romer, L.H., Kang, S.H. & Gracias, D.H. (2019). Direct ink writing of poly (tetrafluoroethylene)(PTFE) with tunable mechanical properties. *ACS applied materials & interfaces*, *11*(31), 28289–28295. DOI: 10.1021/acsami.9b07279

Kaliampakou, C., Lagopati, N., & Charitidis, C.A. (2023). Direct ink writing of alginate–gelatin hydrogel: An optimization of ink property design and printing process efficacy. *Applied Sciences*, *13*(14), 8261. DOI: 10.3390/app13148261

Khan, S.A., Ahmad, H., Zhu, G., Pang, H., & Zhang, Y. (2024). Three-dimensional printing of hydrogels for flexible sensors: a review. *Gels*, *10*(3), 187. DOI: 10.3390/gels10030187

Le, H.T., & Tran, V.T. (2025). A study on the weldability of tough alginate–poly (acrylic acid) hydrogels. *Journal of Polymer Research*, *32*(9), 1–16. DOI: 10.1007/s10965-025-04542-6

Lee, K.Y. & Mooney, D.J. (2001). Hydrogels for Tissue Engineering. Chemical Reviews, Chemical reviews, 101(7), 1869–1880. DOI: 10.1021/cr000108x

Liu, Q., Li, Q., Xu, S., Zheng, Q., & Cao, X. (2018). Preparation and properties of 3D printed alginate–chitosan polyion complex hydrogels for tissue engineering. *Polymers*, *10*(6), 664. DOI: 10.3390/polym10060664

Liu, J., Garcia, J., Leahy, L. M., Song, R., Mullarkey, D., Fei, B., Dervan, A., Shvets, I.V., Stamenov, P., Wang, W., O'Brien, F. J., Coleman, N.C. & Nicolosi, V. (2023). 3D printing of multifunctional conductive polymer composite hydrogels. *Advanced Functional Materials*, *33*(37), 2214196. DOI: 10.1002/adfm.202214196

Malischewski, M., Adelhardt, M., Sutter, J., Meyer, K., & Seppelt, K. (2016). Isolation and structural and electronic characterization of salts of the decamethylferrocene dication. *Science*, *353*(6300), 678–682. DOI: 10.1126/science.aaf6362

Mredha, M.T.I., Tran, V.T., Jeong, S.G., Seon, J.K., & Jeon, I. (2018). A diffusion-driven fabrication technique for anisotropic tubular hydrogels. *Soft Matter*, *14*(37), 7706–7713. DOI: 10.1039/c8sm01235k

Nguyen, T.T., Pham, N.H., Tran, H.S., Cao, L.N., Pham, T.H.N., Phan, Q.B., & Tran, V.T. (2024). Hydrogel 3D printing with direct and indirect extruder. *Mechanical Engineering Advances*, *2*(2), 1470–1470. DOI: 10.59400/mea.v2i2.1470

Singamneni, S., Behera, M.P., Truong, D., Le Guen, M.J., Macrae, E., & Pickering, K. (2021). Direct extrusion 3D printing for a softer PLA-based biopolymer composite in pellet form. *Journal of Materials Research and Technology*, *15*, 936–949. DOI: 10.1016/j.jmrt.2021.08.044

Sun, J. Y., Zhao, X., Illeperuma, W.R., Chaudhuri, O., Oh, K.H., Mooney, D.J., Vlassak , J.J & Suo, Z. (2012). Highly stretchable and tough hydrogels. *Nature*, *489*(7414), 133–136. DOI: 10.1038/nature11409

Tabriz, A.G., Hermida, M.A., Leslie, N.R., & Shu, W. (2015). Three-dimensional bioprinting of complex cell laden alginate hydrogel structures. *Biofabrication*, *7*(4), 045012. DOI: 10.1088/1758-5090/7/4/045012

Tran, V.T., Xu, X., Mredha, M.T.I., Cui, J., Vlassak, J.J., & Jeon, I. (2018). Hydrogel bowls for cleaning oil spills on water. *Water research*, 145, 640–649. DOI: 10.1016/j.watres.2018.09.012

Tran, V.T., Mredha, M.T.I., & Jeon, I. (2020a). High-water-content hydrogels exhibiting superior stiffness, strength, and toughness. *Extreme Mechanics Letters*, 37, 100691. DOI: 10.1016/j.eml.2020.100691

Tran, V.T., Mredha, M.T.I., Na, J.Y., Seon, J.K., Cui, J., & Jeon, I. (2020b). Multifunctional poly (disulfide) hydrogels with extremely fast self-healing ability and degradability. *Chemical Engineering Journal*, 394, 124941. DOI: 10.1016/j.cej.2020.124941

Tran, V.T., Nguyen, T.C., Nguyen, T.T., & Nguyen, H.N. (2023). Environmentally friendly plastic boats–A facile strategy for cleaning oil spills on water with excellent efficiency. *Environmental Science and Pollution Research*, *30*(26), 68848–68862. DOI: 10.1007/s11356-023-26978-3

Tran, V.T. (2024). Anisotropic Ca-alginate hydrogels with superior mechanical properties and excellent stability for underwater applications. *Journal of Polymers and the Environment*, *32*(1), 246–259. DOI: 10.1007/s10924-023-02974-z

Tran, V.T., Nguyen, V.T., Nguyen, T.T., Le, H.T., Truong, T.M.C., Huynh, T.G., Nguyen, H.N.M., Nguyen, L.P.N., Nguyen, H.N., Mredha, M.T.I., & Jeon, I. (2024). Air-stable, self-weldable, and tough alginate-based gels: A sustainable alternative to conventional plastics. *Polymer*, 309, 127451. DOI: 10.1016/j.polymer.2024.127451

Tran, V.T. (2025a). Evaluating the effect of strong binding affinity ions on mechanical properties, electrical conductivity, and weldability of conductive alginate-based hydrogels. *Polymer*, 339, 129145. DOI: 10.1016/j.polymer.2025.129145

Tran, V.T. (2025b). An innovative plastic boat utilizing macroscopic openings for efficient oil spill cleanup on water. *Scientific Reports*, *15*(1), 32064. DOI: 10.1038/s41598-025-18159-8

Van Damme, L., Briant, E., Blondeel, P., & Van Vlierberghe, S. (2020). Indirect versus direct 3D printing of hydrogel scaffolds for adipose tissue regeneration. *Mrs Advances*, *5*(17), 855–864. DOI: 10.1557/adv.2020.117

Xiong, X., Chen, Y., Wang, Z., Liu, H., Le, M., Lin, C., Wu, G., Wang, L., Shi, X., Jia, Y.G. & Zhao, Y. (2023). Polymerizable rotaxane hydrogels for three-dimensional printing fabrication of wearable sensors. *Nature communications*, *14*(1), 1331. DOI: 10.1038/s41467-023-36920-3

Yang, B., Zhang, Y., Zhang, X., Tao, L., Li, S., & Wei, Y. (2012). Facilely prepared inexpensive and biocompatible self-healing hydrogel: a new injectable cell therapy carrier. *Polymer Chemistry*, *3*(12), 3235–3238. DOI: 10.1039/C2PY20627G

Zhang, X., Morits, M., Jonkergouw, C., Ora, A., Valle-Delgado, J.J., Farooq, M., Ajdary, R., Huan, S., Linder, M., Rojas, O., Sipponen, M.H., & O¨sterberg, M. (2020). Three-dimensional printed cell culture model based on spherical colloidal lignin particles and cellulose nanofibril-alginate hydrogel. *Biomacromolecules*, *21*(5), 1875–1885. DOI: 10.1021/acs.biomac.9b01745